engineering proceedings

MDPI

Proceeding Paper

Polar-Coded Anti-Jamming Technique over Impulsive Noise Channels †

Ana-Maria Grigoras Oanca [1,*], Mihaela Andrei [2] and Daniela Tarniceriu [1]

[1] Department of Telecommunications and Information Technologies, "Gheorghe Asachi" Technical University of Iasi, 700050 Iasi, Romania; tarniced@etti.tuiasi.ro
[2] Department of Electronics and Telecommunications, "Dunarea de Jos" University of Galati, 800008 Galati, Romania; mihaela.andrei@ugal.ro
* Correspondence: ana-maria.oanca@student.tuiasi.ro
† Presented at the International Conference on Electronics, Engineering Physics and Earth Science (EEPES2026), Bandirma, Turkey, 24–27 June 2026.

Abstract

This paper presents a polar-coded anti-jamming communication system designed to improve reliability and security in channels affected by Gaussian jamming and impulsive α-stable noise. The proposed configuration combines polar decoding with an Anti-Jamming (AJ) mechanism based on Processing Gain (PG). Several configurations, including standalone polar decoding, anti-jamming only, and their combination, are evaluated using Bit Error Rate (BER) versus Signal-to-Jamming Ratio (SJR). Simulation results show that the combined Successive Cancellation List (SCL) decoder with anti-jamming achieves the best performance, offering about a 3 dB gain over standalone SCL decoding. The study also demonstrates improved physical-layer security through enhanced secrecy capacity.

Keywords: polar codes; impulsive noise; anti-jamming; BER; SCL; SC

1. Introduction

The field of wireless communication is continuously evolving, with a wide range of emerging technologies and techniques being developed to address the challenges associated with transmitting information over communication channels.

A way to mitigate some of the disruptions the communication channel may face is to use channel coding. These codes improve the reliability of data transmission over noisy channels by introducing structured redundancy into the transmitted information [1]. This added redundancy allows the receiver to identify and correct transmission errors [1]. A type of code in this category is the polar code, which has emerged as a promising solution. However, despite their strong error-correction performance and increasing adoption in modern communication systems, there is still an area where the application of polar codes is relatively underexplored: mitigating jamming attacks.

Jamming attacks disrupt wireless communication signals, lowering their quality to the point that accurate information cannot be reliably received or reconstructed [2]. Modern 5G networks are particularly open to advanced jamming attacks due to their reliance on high-frequency bands, dense infrastructure, and complex signaling mechanisms, all of which can be exploited by adversaries [3]. To counter these disruptions, we can deploy several anti-jamming strategies designed to keep wireless links stable. These range from classic physical-layer and spatial fixes to modern approaches like AI-driven learning and environment-aware systems.

Academic Editors: Teodor Iliev, Ivaylo Stoyanov, Grigor Mihaylov and Selahattin Kosunalp

Published: 28 August 2026

While time-tested methods, such as power modulation or spreading signals via the Frequency Hopping Spread Spectrum (FHSS) and Direct Sequence Spread Spectrum (DSSS), provide a solid baseline by boosting signal quality, they often struggle to keep pace with today's more sophisticated, fast-changing jamming tactics [4,5]. DSSS systems exploit Pseudo-Noise (PN) sequences and processing gain to separate desired signals from interference, enabling effective suppression of partial-band and single-frequency jamming. However, their performance against wideband interference remains limited [6].

To further improve 5G robustness, we look at the spatial domain. Using Multiple-Input, Multiple-Output (MIMO) and adaptive beamforming, the system can essentially 'aim' its energy toward legitimate receivers and cast nulls toward jammers. This dual action of boosting the signal while suppressing interference makes the network significantly harder to disrupt than traditional, omnidirectional systems [7,8]. More recently, the shift has moved toward intelligent anti-jamming, where Deep Reinforcement Learning (DRL), Deep Neural Networks (DNN), and game theory act as the system's control. Instead of following fixed rules, these frameworks learn on the fly, decoding the patterns of a changing environment. This allows the system to predict interference before it hits and make split-second spectrum decisions with surgical precision [5]. Rather than fighting for space in a contested band, these techniques use adaptive decision-making to pivot toward 'clean' frequencies. It's a strategy of avoidance and optimization that significantly boosts resilience by ensuring we never stay in a compromised channel for long [5]. Looking toward next-generation networks, Reconfigurable Intelligent Surface (RIS)-assisted anti-jamming has emerged as a promising example, where programmable meta-surfaces manipulate electromagnetic wave propagation to redirect the wanted signals and suppress interference, effectively transforming the wireless environment into an active participant in communication security [4].

In this paper, we propose an approach that uses the processing gain introduced by coding to mitigate the impact of jamming and improve the reliability of the received signal. The system is evaluated in terms of BER across different configurations, including Successive Cancellation (SC) and Successive Cancellation List, with and without anti-jamming. The results show that the joint use of SCL decoding and anti-jamming provides a noticeable performance under harsh interference conditions.

Beyond reliability, the system is also analyzed from a security perspective using the secrecy capacity metric. Different scenarios are considered, including variations in transmitting power, jamming intensity, and propagation conditions. The findings show that secure communication is driven by the imbalance between the legitimate receiver and the eavesdropper. Anti-jamming techniques reduce the interference experienced by the intended receiver while leaving the eavesdropper more exposed. The results highlight that combining coding, interference mitigation, and channel asymmetry can effectively improve both communication reliability and security.

2. System Model

The implemented system employs a polar-coded signal combined with Binary Phase Shift Keying (BPSK) modulation, which is transmitted over a communication channel affected by both Gaussian jamming and impulsive α-stable noise. Additionally, a simplified anti-jamming mechanism is incorporated, modelled through processing gain to enhance robustness against interference.

At the receiver side, signal detection and decoding are done using SC and SCL decoding, applied independently to evaluate their respective performance under the channel conditions.

https://doi.org/10.3390/engproc2026154011

The proposed system starts with a polar encoder, which applies a short block-length polar code to a sequence of information bits, and a block of information of K bits is transformed into a codeword of length N by combining the input vector with a generator matrix and a predefined frozen set. The way the system works is also shown in Figure 1. The diagram was created using diagram.net, a web-based diagramming software, version 31.x.

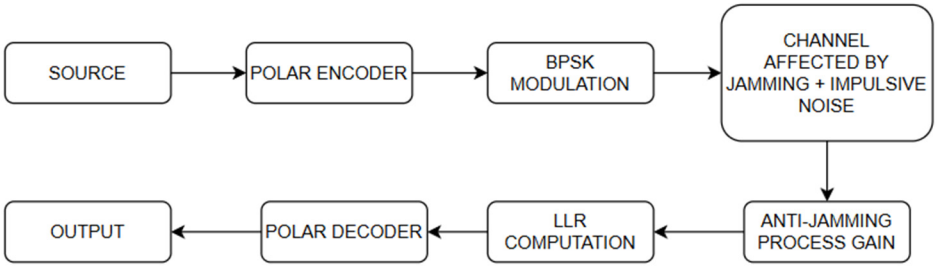

Figure 1. System configuration block diagram.

Through channel polarization, the encoder separates the transmission channels into reliable and unreliable ones. The most reliable K positions are assigned information bits, while the remaining $(N - K)$ positions are filled with frozen bits, typically set to zero.

The encoding binary sequence is obtained as:

$$c = uG_N \tag{1}$$

where:

- $N = 2^n$ is the block length;
- $u \in \{0,1\}^N$ contains the information and frozen bits;
- $G_N = F^{\oplus n}$ is the generator matrix;
- $F = \begin{bmatrix} 1 & 0 \\ 1 & 1 \end{bmatrix}$;
- $n = \log_2 N$.

After the encoded $c[n] \in \{0,1\}$ bits are mapped to BPSK symbols, each bit is converted according to Formula (2). This prepares the signal for transmission in baseband form.

$$x[n] = 1 - 2c[n], \qquad x[n] \in \{-1, +1\} \tag{2}$$

2.1. Channel and Interference Model

The transmitted signal propagates through a channel affected not only by noise but also by intentional interference (jamming) and impulsive perturbation. First, we introduced a Gaussian jammer, modelled as a random process with variance determined by the SJR; then in the system, impulsive noise is added, modelled using a Symmetric α-Stable (SαS) distribution. The impulsive noise is controlled by two parameters: the stability parameter α, which determines the heaviness of the distribution tails, and the dispersion parameter γ, which controls the overall intensity. The received signal can therefore be expressed as:

$$y[n] = x[n] + j[n] + \eta_\alpha[n] \tag{3}$$

where:

- $j[n]$ is Gaussian jamming;
- $\eta_\alpha[n]$ is impulsive α-stable noise.

https://doi.org/10.3390/engproc2026154011

The first component is Gaussian jamming, representing intentional interference. It is modelled as:

$$j[n] \sim \mathcal{N}\left(0, \sigma_J^2\right), \tag{4}$$

where the variance is determined by the SJR:

$$\sigma_J^2 = 10^{-SJR_{dB}/10}. \tag{5}$$

This type of interference is broadband and affects all transmitted symbols. The second component is impulsive noise, modelled using a symmetric α-stable distribution:

$$\eta_\alpha[n] \sim S\alpha S(\alpha, \gamma), \tag{6}$$

where:

- $0 < \alpha < 2$, controlling the heaviness of the distribution tails;
- $\gamma > 0$, representing the dispersion parameter.

Unlike Gaussian noise, α-stable noise produces occasional high-amplitude spikes, making the channel strongly non-Gaussian and more difficult to handle [9].

In this paper, the impulsive noise is assumed to be symmetric, with zero skewness and zero location parameter. For the simulations, the noise samples are generated using the Chambers–Mallows–Stuck (CMS) method, such as in [10], which provides an efficient way to simulate α-stable random variables. And as such, the noise samples are obtained as:

$$\eta_\alpha = \gamma \cdot \frac{\sin(\alpha U)}{(cosU)^{\frac{1}{\alpha}}} \cdot \left(\frac{\cos(U - \alpha U)}{W}\right)^{\frac{1-\alpha}{\alpha}}, \tag{7}$$

where:

$$U \sim \mathcal{U}\left(-\frac{\pi}{2}, \frac{\pi}{2}\right), W \sim \text{Exp}(1). \tag{8}$$

2.2. Anti-Jamming Method

To mitigate the effect of jamming, the system incorporates a simplified AJ mechanism based on PG. The PG introduced by polar coding can be interpreted as an implicit spreading mechanism, analogous to the processing gain in direct-sequence spread spectrum systems, meaning in our case the ratio between encoded and information bits:

$$G = N/K. \tag{9}$$

This puts in place a direct connection between channel coding and spread-spectrum principles, where redundancy in the coded domain plays a similar role to bandwidth expansion in DSSS systems. It can also be expressed in decibels as:

$$G_{dB} = 10\log\left(\frac{N}{K}\right). \tag{10}$$

However, the linear form is used in the Signal-to-Interference-plus-Noise Ratio (SINR) and secrecy capacity calculations. This gain is used to reduce the power of the Gaussian jammer:

$$\sigma_{J,\text{AJ}}^2 = \frac{\sigma_J^2}{10^{G_{dB}/10}}. \tag{11}$$

As a result, the received signal under anti-jamming becomes:

$$y_{\text{AJ}}[n] = x[n] + j_{\text{AJ}}[n] + \eta_\alpha[n]. \tag{12}$$

It is important to note that this mechanism affects only Gaussian interference, while the impulsive noise remains unchanged [11]. Because of this, two scenarios are considered: one without anti-jamming (full jammer power) and another one with anti-jamming (reduced Gaussian jammer power).

In the combined system, decoding is applied after anti-jamming. For the SC-based combined scheme, the reduced jammer power improves the quality of the input LLRs, which directly benefits the SC decoding process. As for the SCL-based combined scheme, the benefits of anti-jamming are further enhanced by SCL decoding since SCL maintains multiple candidate paths.

2.3. Polar Decoding

The system employs two decoding strategies: Successive Cancellation and Successive Cancellation List. At the receiver, the corrupted signal is first converted into soft reliability values, expressed as Log-Likelihood Ratios (LLRs). These are computed using a simplified Gaussian approximation as in Formula (13). The effective noise variance is approximated as the sum of the Gaussian jammer variance and the impulsive noise dispersion, as in Formula (14) for the case without anti-jamming and as in Formula (15) for the case with anti-jamming.

$$L[n] = ln\frac{P\left(y[n] \mid x[n] = +1\right)}{P\left(y[n] \mid x[n] = -1\right)} \approx \frac{2y[n]}{\sigma^2_{\text{eff}}} \tag{13}$$

Although the actual channel is non-Gaussian, this approximation allows for practical implementation of polar decoding:

$$\sigma^2_{\text{eff}} = \sigma^2_J + \gamma, \tag{14}$$

$$\sigma^2_{\text{eff}} = \sigma^2_{J,AJ} + \gamma. \tag{15}$$

2.3.1. Successive Cancellation

In SC decoding, the bits are estimated sequentially, starting from the first position. Each decision is made based on the received signal and all previously decoded bits; frozen bits are fixed, while information bits are decided one by one [12].

For each bit i, the decision rule is:

$$\hat{u}_i = \begin{cases} 0, \ i \in F; \\ 0, \ i \notin F, \ L_i \geq 0; \\ 1, \ i \notin F, L_i < 0. \end{cases} \tag{16}$$

where:

- $\mathcal{F} \subset \{0, \ 1, \ldots, \ N-1\}$, is the frozen set of bits;
- L_i is the LLR for bit i.

The LLRs are computed recursively using:

$$f(a,b) \approx sign(a)sign(b)min(\mid a \mid, \mid b \mid), \tag{17}$$

$$g(a,b,\hat{u}) = b + (1-2\hat{u})a, \tag{18}$$

where:

- a is the LLR from the left branch;
- b is the LLR from the right branch;
- $\hat{u}_i$ is the previously decoded bit.

https://doi.org/10.3390/engproc2026154011

2.3.2. Successive Cancellation List

To improve performance, the system also uses SCL decoding, which extends SC by maintaining multiple candidate decoding paths.

Instead of making a single decision at each step, the decoder considers both possibilities and keeps the most reliable paths. At the end of the process, the best candidate is selected. This approach significantly improves robustness, especially in difficult channel conditions such as those with impulsive noise [13].

SCL decoding improves SC by maintaining multiple decoding paths. For each bit, each path is extended with both 0 and 1, and the best L paths are retained. The path metric is updated as:

$$PM_i = PM_{i-1} + ln\left(1 + e^{-(1-2u_i)L_i}\right) \tag{19}$$

At the end of the decoding process, the most reliable candidate sequence is selected as:

$$\hat{u} = arg\ min\ PM \tag{20}$$

where û is the estimated information vector.

SC decoding has relatively low computational complexity, on the order of $\mathcal{O}(N\log N)$, making it suitable for practical low-latency implementations. However, its sequential decoding structure makes it more sensitive to error propagation. In contrast, SCL decoding exhibits higher computational complexity, approximately $\mathcal{O}(LN\log N)$, due to the maintenance of multiple decoding paths. This is illustrated in Figure 2, where the computational complexity of the two decoding algorithms is evaluated for different block lengths. Nevertheless, this additional complexity enables significantly improved decoding performance and robustness, especially in highly impulsive and jammed environments. These results emphasize the trade-off between decoding complexity and communication reliability.

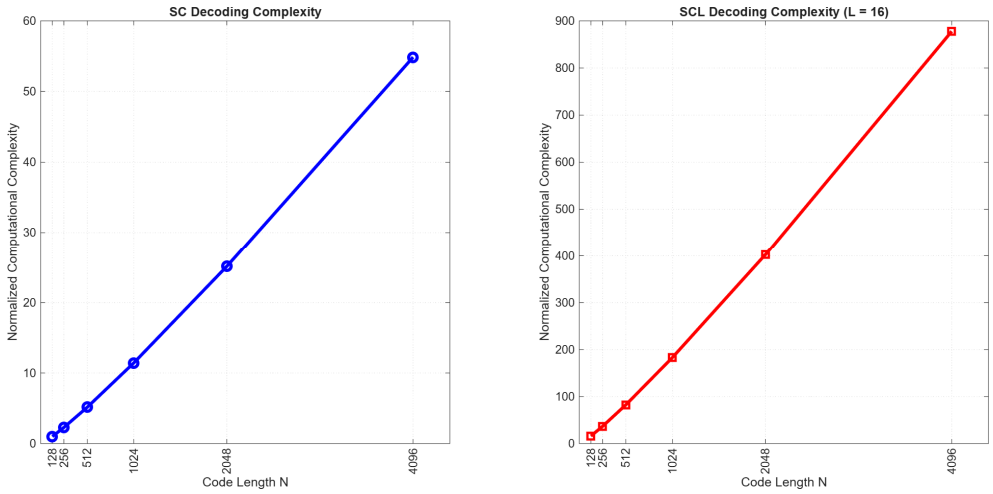

Figure 2. Complexity comparison between SCL and SC decoding.

3. Secrecy Capacity

Secrecy capacity is an important component in physical-layer security, which at its core is the maximum rate at which information can be transmitted securely over a wireless channel in the presence of an eavesdropper. It is expressed as:

$$C_s = max(0, C_B - C_E) \tag{21}$$

where:

- C_B is the capacity of the legitimate channel (Bob);
- C_E is the capacity of the eavesdropper channel (Eve).

It is also defined as the positive difference between the capacity of the legitimate communication link and that of the eavesdropper link, meaning secure communication is achievable only when the legitimate receiver experiences a better channel than the eavesdropper [14].

In interference-limited environments, these capacities are modelled using Shannon's formula, $C = \log_2(1 + \text{SINR})$, with the SINR incorporating both jamming and impulsive noise effects. Techniques such as friendly jamming and power allocation are therefore used to reduce the eavesdropper's channel quality while maintaining acceptable performance at the legitimate receiver [15].

The considered system is evaluated in terms of secrecy capacity based on three complementary models: source power-based, SJR-based, and path-loss.

3.1. Source Power-Based Model

For the source power-based model, both receivers experience the same transmit power, and the asymmetry is introduced through the processing gain $G = N/K$, which reduces the effective jamming at the legitimate receiver as in Formulas (22) and (23). In this case, secrecy is achieved by interference mitigation at the legitimate receiver.

$$C_B = log_2\left(1 + \frac{P_s}{\frac{P_{jam1}}{G} + \gamma}\right), \tag{22}$$

$$C_E = log_2\left(1 + \frac{P_s}{P_{jam1} + \gamma}\right), \tag{23}$$

where:

- P_s is the transmit power;
- $P_{jam1} = 10^{P_{jam1,\,dB}/10}$, is the jamming power;
- G is the processing gain from anti-jamming;
- γ is the impulsive noise dispersion.

3.2. Signal-to-Jamming Ratio-Based Model

In the SJR-based model, the jamming power is controlled through jamming power as in Formula (24), and the capacities become those in Formulas (25) and (26).

$$P_{jam2} = 10^{-\text{SJR}_{dB}/10} \tag{24}$$

Here, the SJR acts as a control parameter that directly influences the interference level and highlights the transition between low- and high-interference regimes.

$$C_B = log_2\left(1 + \frac{1}{\frac{P_{jam}}{G} + \gamma}\right) \tag{25}$$

$$C_E = log_2\left(1 + \frac{1}{P_{jam} + \gamma}\right) \tag{26}$$

https://doi.org/10.3390/engproc2026154011

3.3. Path-Loss Model

For the final model, the path-loss model, spatial asymmetry is introduced through distance-dependent attenuation:

$$P_{r,B} = \frac{P_s}{d_B^{\eta}}, \tag{27}$$

$$P_{r,E} = \frac{P_s}{d_E^{\eta}}, \tag{28}$$

where:

- d_B is the distance from the transmitter to Bob;
- d_E is the distance from the transmitter to Eve;
- η is the path-loss exponent that characterizes the propagation environment.

In this case, the capacity is as shown in Formulas (29) and (30).

$$C_B = log_2\left(1 + \frac{P_{r,B}}{\frac{P_{jam1}}{G} + \gamma}\right) \tag{29}$$

$$C_E = log_2\left(1 + \frac{P_{r,E}}{P_{jam1} + \gamma}\right) \tag{30}$$

A smaller d_B relative to d_E provides a natural advantage to the legitimate receiver. In this case, secrecy is reinforced when the legitimate receiver is closer to the transmitter ($d_B < d_E$).

4. Results

In this section, we present the simulation results and evaluate the proposed system from both reliability and security perspectives. All the simulations in this paper were done using MATLAB 2026a.

First, the performance of the proposed configuration is analyzed and compared with benchmark schemes, namely, standalone polar code decoders (SC and SCL) and a conventional anti-jamming technique. The evaluation is carried out over a communication channel affected by both Gaussian jamming and impulsive α-stable noise to assess system robustness in terms of BER. In addition, the Power Spectral Density (PSD) of the transmitted signal and interference components is analyzed to provide further insight into the impact of the anti-jamming mechanism.

Secondly, the same system is examined from a physical-layer security standpoint using the secrecy capacity. This analysis investigates how parameters such as transmitting power, jamming intensity, and channel asymmetry influence the achievable secure transmission rate.

4.1. Polar-Coded Anti-Jamming System

The Polar code used in the proposed system is characterized by the parameters $N = 256$ and $K = 128$, resulting in a coding rate $R = K/N = 0.5$. Simulations are conducted over a channel affected by both Gaussian jamming and impulsive α-stable noise, with parameters $\alpha = 1.5$ and $\gamma = 0.05$.

Five scenarios are considered and evaluated in terms of bit error rate as a function of the signal-to-jamming ratio:

1. Polar code SC decoding;
2. Polar code SCL decoding;
3. Processing gain anti-jamming;

4. Combined polar code SC decoding with anti-jamming;
5. Combined polar code SCL decoding with anti-jamming.

The number of paths for the SCL decoding, for scenarios 2 and 5, is set at $L = 16$. The results presented in Figure 3 show that reducing Gaussian interference before decoding significantly enhances the reliability of the information that was received, thereby improving the performance of polar decoders, particularly SCL decoding. In contrast, the standalone anti-jamming approach remains limited by the presence of impulsive α-stable noise, which may significantly degrade BER performance due to its burst-like interference characteristics. Furthermore, although SCL decoding achieves superior robustness and error-correction capability compared with SC decoding, this improvement comes at the cost of increased computational complexity, as shown in Figure 2, as well as higher memory usage and processing latency for larger list sizes.

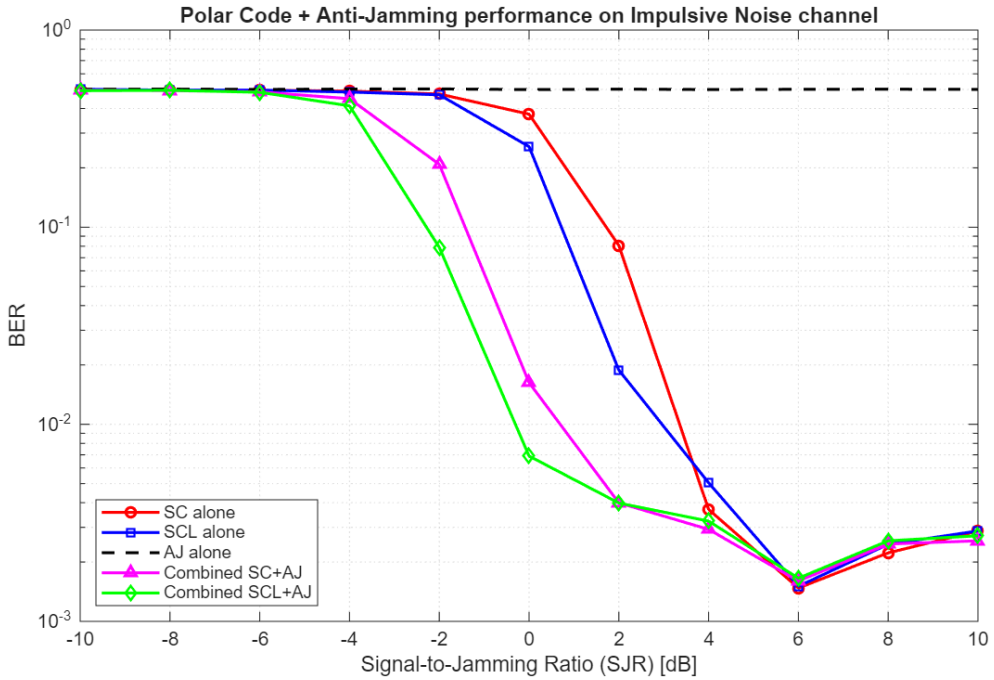

Figure 3. Performance of the configurations over the Gaussian jamming and impulsive channels.

We also observed that the combined polar SCL decoding with anti-jamming achieves a coding gain of approximately 3 dB compared to the standalone SCL decoder. The improvement is due to the reduction in the effective jamming power before decoding, which increases the SINR at the receiver.

The PSD is illustrated in Figure 4, where three cases are compared: the useful polar-coded signal, the total interference without anti-jamming, and the interference after applying the anti-jamming mechanism.

The useful signal exhibits a relatively flat spectrum. In contrast, the interference without anti-jamming shows significantly higher power across the entire frequency band. After applying the anti-jamming technique, a noticeable reduction in interference power is observed, which effectively suppresses the Gaussian component of the jammer.

https://doi.org/10.3390/engproc2026154011

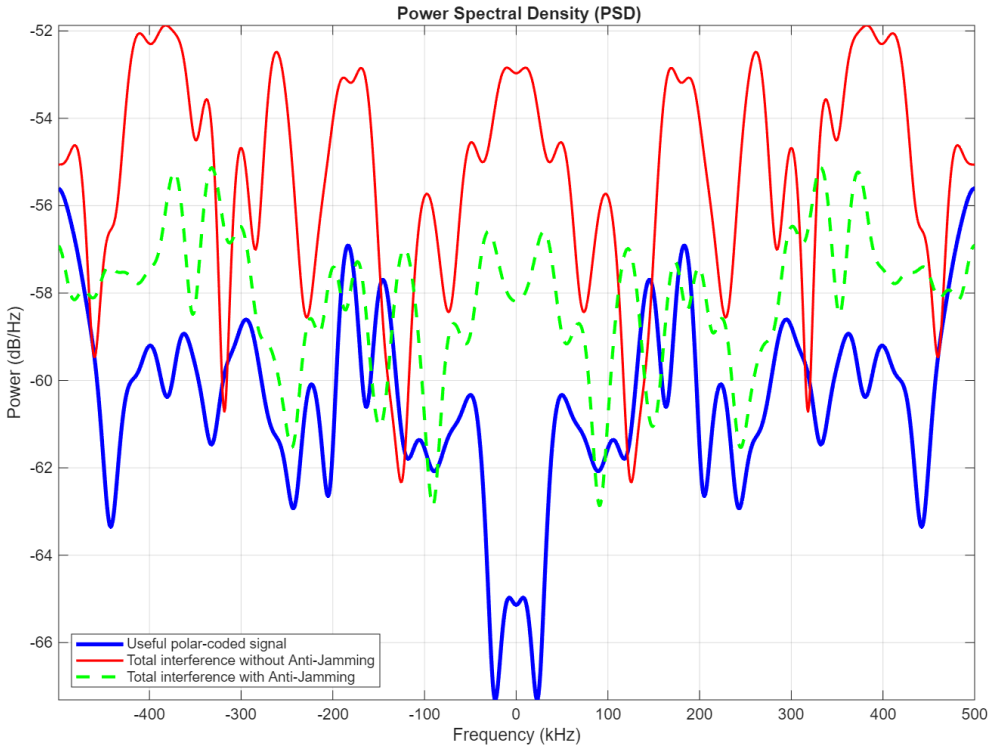

Figure 4. Power Spectral Density evaluation.

4.2. Secrecy Capacity

In this subsection, the proposed system is further evaluated for physical-layer security, using the secrecy capacity. The analysis considers multiple scenarios, including variations in transmitting power, SJR, and path loss. The results can be observed in Figure 5, and they follow the same trend observed in the BER performance of the polar-coded anti-jamming system.

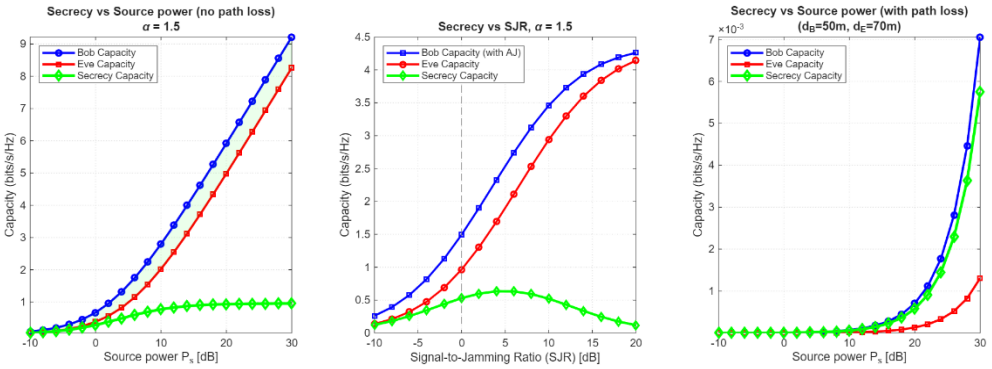

Figure 5. Secrecy capacity evaluation for the proposed system.

In the first scenario (pictured on the left), secrecy capacity is evaluated as a function of the source power without considering path loss ($\eta = 3$). Both the legitimate receiver and the eavesdropper benefit from an increase in transmit power. The results also show that the legitimate receiver consistently benefits from the anti-jamming mechanism, which reduces interference before decoding. Consequently, the secrecy capacity stays positive over most of the evaluated range and increases steadily as the transmit power grows.

In the second scenario (pictured in the middle), where secrecy capacity is analyzed as a function of the SJR, the impact of the anti-jamming mechanism becomes more evident. At low SJR levels, both the legitimate receiver and the eavesdropper experience performance degradation due to interference; the impact is noticeably stronger on the eavesdropper.

https://doi.org/10.3390/engproc2026154011

In the third scenario (shown on the right), the inclusion of path loss leads to more stable secrecy performance by introducing additional spatial asymmetry between the two receivers. Because the legitimate receiver is closer to the transmitter ($d_B = 50$ m), it benefits from a stronger received signal, further enhancing the advantage already gained through the anti-jamming mechanism.

5. Conclusions

This paper analyses the performance and security of a polar-coded anti-jamming communication system operating in the presence of Gaussian jamming and impulsive α-stable noise. The BER and spectral analysis show that the combined use of polar coding and anti-jamming significantly improves the strength of the transmitted signal under harsh interference conditions. Mitigating Gaussian interference before decoding allows polar decoders to perform more efficiently, with the SCL decoder delivering the strongest results among the tested configurations.

The simulations show that the proposed combined configuration achieves a coding gain of about 3 dB compared to a standalone polar SCL decoder, along with a slight additional improvement over the other configurations. This is further supported by the PSD analysis. Without anti-jamming, interference spreads across the full frequency band at high power levels, whereas applying the anti-jamming technique significantly attenuates the Gaussian jammer component, resulting in a cleaner received signal.

When it comes to the security aspect, the secrecy capacity analysis indicates that the achievable secure rate is largely determined by the asymmetry between the legitimate and eavesdropping channels. The results show that anti-jamming consistently benefits the legitimate receiver, especially under strong interference, and incorporating path loss adds a spatial advantage.

Author Contributions: Conceptualization, methodology, software, validation, formal analysis, investigation, resources, data curation, writing—original draft preparation, A.-M.G.O., M.A. and D.T.; writing—review and editing, visualization, A.-M.G.O. and M.A.; supervision, D.T.; project administration, A.-M.G.O. and M.A. All authors have read and agreed to the published version of the manuscript.

Funding: This research received no external funding.

Institutional Review Board Statement: Not applicable.

Informed Consent Statement: Not applicable.

Data Availability Statement: Any data not contained within this article can be provided by authors on request.

Conflicts of Interest: The authors declare no conflicts of interest.

Abbreviations

The following abbreviations are used in this manuscript:

BER	Bit Error Rate
SJR	Signal-to-Jamming Ratio
SCL	Successive Cancellation List
FHSS	Frequency Hopping Spread Spectrum
DSSS	Direct Sequence Spread Spectrum
PN	Pseudo-Noise
MIMO	Multiple-Input, Multiple-Output

DRL	Deep Reinforcement Learning
DNN	Deep Neural Networks
RIS	Reconfigurable Intelligent Surfaces
SC	Successive Cancellation
BPSK	Binary Phase Shift Keying
SαS	Symmetric α-Stable
PG	Processing Gain
AJ	Anti-Jamming
LLR	Log-Likelihood Ratios
SINR	Signal-to-Interference-plus-Noise Ratio
PSD	Power Spectral Density

References

1. Li, C.; Zhong, M.; Zhang, Y.; Song, D.; Zhang, N.; Yang, J. Network coding-enhanced polar codes for relay-assisted visible light communication systems. *Entropy* **2024**, *26*, 1112. [CrossRef] [PubMed]
2. Ma, D.; Wang, Y.; Wu, S. Against jamming attack in wireless communication networks: A reinforcement learning approach. *Electronics* **2024**, *13*, 1209. [CrossRef]
3. Holguin, O.; Donati, R.; Natanzi, S.B.H.; Tang, B. A MUSIC-based adaptive beamforming approach for mobile jamming mitigation in 5G networks. In Proceedings of the IEEE Military Communications Conference (MILCOM 2025), Los Angeles, CA, USA, 6–10 October 2025.
4. Tariq, Z.U.A.; Baccour, E.; Erbad, A.; Hamdi, M. RIS assisted anti-jamming in next-generation wireless communication networks: A survey of threats, solutions, and research challenges. *IEEE Open J. Commun. Soc.* **2025**, *6*, 8714–8744. [CrossRef]
5. Cao, W.; Chu, F.; Jia, L.; Zhou, H.; Zhang, Y. A multi-agent deep reinforcement learning anti-jamming spectrum-access method in LEO satellites. *Electronics* **2025**, *14*, 3307. [CrossRef]
6. Wang, X.; Zhou, Q. Analytical technique leveraging processing gain for evaluating the anti-jamming potential of underwater acoustic direct sequence spread spectrum communication systems. *Symmetry* **2023**, *15*, 1710. [CrossRef]
7. Tsachrelias, K.; Katsigiannis, C.-A.; Kokkinos, V.; Bouras, C.; Gkamas, A.; Pouyioutas, P. Robust protection of 5G MIMO networks from jamming attacks via adaptive beamforming. *Procedia Comput. Sci.* **2025**, *265*, 65–72. [CrossRef]
8. Pirayesh, H.; Zeng, H. Jamming attacks and anti-jamming strategies in wireless networks: A comprehensive survey. *IEEE Commun. Surv. Tutor.* **2022**, *24*, 767–809. [CrossRef]
9. Clavier, L.; Peters, G.W.; Septier, F.; Nevat, I. Impulsive noise modeling and robust receiver design. *J. Wirel. Commun. Netw.* **2021**, *2021*, 13. [CrossRef]
10. Duan, S.; Fang, J.; Xue, H.; Li, J. Research on spectrum sensing algorithms under impulsive noise. *Electronics* **2026**, *15*, 912. [CrossRef]
11. Gui, G.; Xu, L.; Ma, W.; Chen, B. Robust adaptive sparse channel estimation in the presence of impulsive noises. In Proceedings of the IEEE International Conference on Digital Signal Processing (DSP), Singapore, 21–24 July 2015.
12. Wu, C.-J.; Lin, C.-Y.; Huang, Y.-C. Polar coding and early SIC decoding for uplink heterogeneous NOMA. *Entropy* **2025**, *27*, 1167. [CrossRef] [PubMed]
13. Rowshan, M.; Viterbo, E. SC list-flip decoding of polar codes by shifted pruning: A general approach. *Entropy* **2022**, *24*, 1210. [CrossRef] [PubMed]
14. Zhao, H.; Zhao, G.; Wang, X.; Zhang, Z.; Xun, X. Intelligent anti-jamming communication technology with electromagnetic spectrum feature cognition. *PLoS ONE* **2025**, *20*, e0319953. [CrossRef] [PubMed]
15. Hayajneh, M.; Gulliver, T.A. Secrecy capacity in two-way energy harvesting relay networks with a friendly jammer. *Wirel. Netw.* **2021**, *27*, 4551–4566. [CrossRef]